Near-Field Influence on Barrier Evolution in Symmetric Atom Transfer Reactions: A New Model for Two-State Mixing†

Heather A. Rypkema,* Neil M. Donahue,‡ and James G. Anderson

Department of Chemistry and Chemical Biology, Harvard University, Cambridge, Massachusetts 02138

Received: July 5, 2000; In Final Form: October 3, 2000

We here consider the fundamental interactions which drive barrier evolution in atom transfer reactions. By applying the functional behavior predicted by second-order nondegenerate perturbation theory to a symmetric linear curve crossing model, we are able to derive a simple formula for two-state mixing in the near-field. It becomes readily apparent that the system property most critically responsible for governing the magnitude of coupling is the diabatic state-to-state overlap. In order to explore this parameter in depth, we outline a basic strategy for diabatic state construction in the near-field and use the imposed symmetry requirements and phase relations to derive a functional form which relates the state-to-state overlap to molecular orbital properties of the isolated reactants and the interatomic overlap matrix. Finally, we show how trends in barrier heights may be analyzed in the context of combined far-field and near-field effects and how these effects may be separated in order to provide insight into the underlying physics and broadly applicable mechanistic information.

Introduction

The potential energy surface is the landscape upon which all chemical interactions occur, yet much of our conception of the forces which shape these surfaces is caught up in the numerical complexity of the many electron quantum mechanical system. Even the basic atom transfer, one of the simplest bimolecular reactions, is not wholly understood. While it is well-known that these reactions are governed by the barrier to abstraction, there remain a multitude of unanswered questions concerning the fundamental physics that produce those barriers. Rates for simple atom transfer reactions span many orders of magnitude, indicating a substantial variation in barrier height from system to system. Such variance in reactivity is attributable to myriad causes, indistinguishable based on information about the barrier heights alone. In order to comprehend the physical principles which govern these important reactions, it is necessary to develop a model that can explain the observed reactive trends in terms of relevant, measurable properties of a chemical system.

The advent of computational quantum chemistry has provided today's physical chemist with a heretofore unattainable capacity for calculating the energy surfaces of complex systems. As computer technology soars in speed and plummets in price, the computational power of electronic structure calculations will doubtlessly become both more accurate and more widely utilized. However, there is also substantial scientific value to a simpler approach. Basic analytical models, while significantly less accurate, have the distinct advantage of demonstrating explicitly how a multitude of independent variables combine to yield the ultimate solution. Not only does such a model result in a stronger understanding of the underlying physics, but it also allows for the tailoring of experiments with the specific aim of either supporting or refuting its predictions.

Thus, on the opposite end of the complexity spectrum from the intensive computational techniques lies our approach to fundamental reactivity theory. The aim is not to attain numerical accuracy on barrier height prediction for a single chemical system but rather to explain trends in terms of causality, identifying the systemic properties which *create* those trends. To this end, we seek to develop a general model for chemical reactivity that permits us to isolate the distinct parameters which shape the potential energy surface and to evaluate the relative importance of each, thereby lending insight into the physical mechanisms involved.

Fundamentals of the Model

Development of this model was motivated by the desire to calculate barrier heights with an emphasis on facility and a focus on reproducing chemical trends rather than predictive accuracy. Its purpose is to isolate individual aspects of a system in order to assess their relative significance in barrier height control. As such we concentrate on the impact of first-order effects, neglecting higher order terms which have only a minor comparative influence on the shape of the potential energy surface.

In this work, we shall focus specifically on atom transfer, a basic but highly prevalent family of reactions. It has long been understood[1] that the barriers of such reactions arise from diabatic state mixing, but while the problem has been studied extensively,[2−14] analytical solutions in terms of measurable system properties have been a rarity. Shaik et al.[9] have derived a solution which demonstrates that the coupling of two states is dependent upon the state-to-state overlap and elements of the interatomic overlap matrix. The derivation we shall present agrees with that variable dependence, but considers the problem for a completely general interaction potential.

In order to bridge the conceptual gap between empirical reactivity trends and the physical phenomena which drive them, we have sought to develop an approach to thinking about two-state crossing reactions with the ultimate goal of elucidation via simplification, emphasizing the isolation of the controlling physics rather than a numerically precise predictive capacity.

† Part of the special issue "Harold Johnston Festschrift".

* Corresponding author. E-mail: ryp@huarp.harvard.edu.

‡ Present address: Departments of Chemistry and Chemical Engineering, Carnegie Mellon University, Pittsburgh, PA, 15217.

10.1021/jp002393u CCC: $20.00
Published on Web 12/20/2000

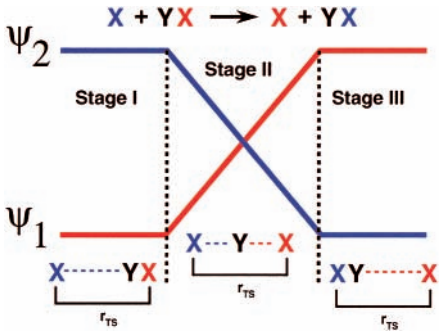

Figure 1. Basic three-stage linear curve-crossing model. Over the course of the atom transfer, the states ψ_1 (corresponding to the reactant ground state) and ψ_2 (corresponding to the product ground state) invert in energy. The X−X bond distance remains constant throughout the transfer.

Beginning with the approximation that the diabatic states evolve linearly over the atom transfer region, we shall derive a simple method for estimating the two state mixing and thereby identify the systemic parameters which contribute to barrier height formation.

The first important assumption of the linear curve crossing problem is that the adiabatic barrier height may be represented as a fraction of the crossing height, thereby separating the absolute energy scale from the coupling. Mathematically, this is expressed as

$$E_b = E_x(1 - \beta) \tag{1}$$

where E_x is the diabatic crossing height and β is a parameter arising from near-field state mixing. The former quantity is easily calculable using a linear crossing model and depends on far-field properties of the system, in particular the nature of the dominating excited state at the boundary.[15] Accurate calculation of the latter quantity, β, is significantly more difficult and the goal of this paper is the substantial simplification thereof.

In the following sections we shall briefly address the fundamental approach to calculating E_x and present our derivation of β. For the sake of clarity, only the symmetric curve-crossing case will be presented here; the asymmetric solution shall be presented in the future.

Linear Crossing Approximation. In order to quickly simplify the barrier calculation we shall treat the electron-transfer process as an elementary two state linear curve crossing.

The reaction is divided into three stages as described by Donahue et al.[15] and depicted for an elementary, symmetric atom abstraction in Figure 1. Stage I represents pure reactants; ψ_1 is the lower surface, corresponding to the occupied frontier molecular orbital of the reactants while ψ_2, which maps onto the product ground state, represents the excited state. Naturally, in Stage III the roles of the wave functions are reversed, with ψ_2 corresponding to the ground state and ψ_1 the excited state. In general, we model Stages I and III as undistorted approach and withdrawal, localizing all molecular distortions to Stage II. In the case of an atom abstraction, Stage I represents the approach of the abstracting species, ending when the X−X bond distance is equal to its value at the transition state, as indicated in Figure 1. In Stage II, the abstracted species is transferred from one atom to the other, passing through the transition state geometry, while the X−X bond distance remains fixed. Finally, Stage III represents withdrawal of product species.

For the purpose of this study, we have not made any assumptions about the nature of the state interaction in the far-field. However, it is presumed that at the Stage II boundaries, coupling of the two states may be adequately described by the prediction of nondegenerate two-state perturbation theory. The resultant energy will provide us with a boundary condition for our predicted adiabatic energy.

This basic linear crossing model provides the framework for our coordinate system. The variable ρ is the reduced reaction coordinate for Stage II, taking on a value of -1 for reactants and $+1$ for products. In symmetric reactions such as those considered here, the transition state necessarily occurs at $\rho = 0$. As such, the symmetry of the system allows for an extremely simple expression for the crossing height.

$$E_x = \frac{\Delta E}{2} \tag{2}$$

where ΔE is the energy difference between the diabatic states at the Stage II boundaries.

Please note that while the Stage I and III energies are depicted as constant in Figure 1, this is not necessarily the case. Depending on which excited state is governing the reaction, the far-field energies may evolve in a variety of ways, producing different boundary conditions. We have shown in previous papers[15−17] that this feature of the model may be exploited to better understand the mechanism for radical−molecule reactions by examining the relationship between measured activation barriers and predicted crossing heights. In the case of reactions dominated by the singlet and triplet surface interaction, the far-field splitting is simply determined by $^3/_4$ the singlet−triplet gap.[18] Since the two states are noninteracting at long range, this splitting may be presumed roughly constant throughout regions I and III. In the case of reactions dominated by the ionic surface, the far-field splitting is simply IP−EA and evolves Coulombically until the region II boundary.

While the nature of the controlling excited state plays a critical role in determining the value of E_x, it does not otherwise influence the coupling. Hence in the treatment which follows the crossing height may be presumed totally general, independent of the specific electronic states involved. For the purpose of this study, we shall consider only near-field control of barrier height. Crossing height in this regime can be regarded as a scaling factor which, as will be shown in subsequent derivations, is immaterial to the magnitude of coupling. This separability is a critical part of our model design.

Hyperbolic Approximation. In order to derive a mathematical formulation for β it is necessary to strategically constrain the shape of the potential energy surface in a manner that is both scientifically reasonable and simple enough to avoid obscuring the underlying physics involved. The constraint we have selected is the explicit treatment of the adiabatic surface as a hyperbola, the asymptotes of which are the diabatic energy states, throughout the atom transfer region. The hyperbola is the canonical solution for a two-state avoided crossing problem,[19] and holds a distinct advantage over more common barrier potentials such as Eckhart[20] because it is completely constrained by the initial conditions of the problem and thus does not rely on variable parameters requiring adjustments from an empirical fit to the data. The symmetry of the splitting is readily apparent from the energy correction derived from second order, nondegenerate perturbation theory for a two-level system.

$$E_i = E_i^{(0)} + \frac{H'^{\,2}_{ij}}{E_i^{(0)} - E_j^{(0)}} \tag{3}$$

The assumption that this correction is the dominant effect permits us to apply hyperbolic functional behavior to the resultant adiabatic states.

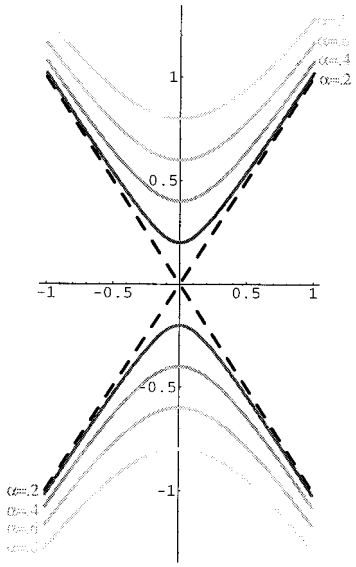

Figure 2. Hyperbolae for a series of α values. At small α the functional surface deviates only slightly from the asymptotes. Splitting is enhanced as α increases.

In order to simplify later calculations, we shall define the origin of our energy scale at the crossing point; the energy of the transition state on the lower adiabatic surface is now given by $-\alpha E_x$, where α is a parameter which is analogous but not necessarily equivalent to β. The slope of the asymptotes is simply given by $\pm E_x$. We may then express our model adiabatic energy as

$$E_{ad}^{hyp} = -E_x(\alpha^2 + \rho^2)^{1/2} \tag{4}$$

Hyperbolae for a series of α values are depicted in Figure 2. Note that smaller values of α correspond to weakly coupled systems, for which the adiabatic state may be closely approximated by the diabatic state for a significant portion of the reaction coordinate. For larger values of α, the splitting is significant, and the diabatic states may be regarded as strongly mixed throughout Stage II.

Having approximated the Stage II PES as a hyperbola, we may now express the near-field barrier height as the difference between the modeled adiabatic energy at the transition state and boundary. Thus

$$E_b = -E_x\alpha - (-E_x(\alpha^2 + 1)^{1/2})$$

$$= E_x((\alpha^2 + 1)^{1/2} - \alpha) \tag{5}$$

We may now relate the splitting parameter, α, to β via eq 1. Solution for β yields

$$\beta = 1 + \alpha - (1 + \alpha^2)^{1/2} \tag{6}$$

Note that by definition α is positive and real, which limits β to values between zero and one. Obviously, the hyperbola is not an appropriate model for describing reactions with negative activation barriers, so this is precisely the range of β we are looking for.

Now that we have established the fundamental premises of this model, let us apply it to a generalized quantum mechanical system.

Quantification of Two-State Coupling

In this section we shall derive a simple formula for calculating the parameter, α. Once known, α may be combined with the crossing height derived from the far-field properties in order to predict the potential barrier resulting from the atom transfer interaction. We have endeavored to maintain maximal generality so that the formulation would be applicable to any symmetric linear curve crossing, regardless of the nature of the excited state.

In the simple methodology of this model, the adiabatic wave function Ψ is expressed as a linear combination of diabatic states, ψ_1 and ψ_2. A constant coupling term is then introduced into the Hamiltonian and the adiabatic energy calculated. The coupling constant, which is needed in order to calculate perturbative splitting, is determined by evaluating the explicit adiabatic energy at the transition state and imposing the hyperbolic value.

Problem Setup. Let us begin by expressing the unnormalized ground state adiabatic wave function as a linear combination of the individual diabatic states.

$$\Psi = \cos\delta\psi_1 - \sin\delta\psi_2 \tag{7}$$

The parameter δ is the familiar mixing angle, and its value is a direct reflection of the extent to which the chemical reaction has occurred. In the context of the three-stage model, we can presume that δ has a value close to zero (pure ψ_1) at the Stage I/Stage II boundary ($\rho = -1$) and a value close to $\pi/2$ (pure ψ_2) at the Stage II/Stage III boundary ($\rho = 1$). Clearly, δ will be exactly equal to $\pi/4$ at the crossing point, thereby reducing eq 7 to the appropriate ground state solution.

In the absence of coupling, eq 7 is fully normalized. However, the presumption of state mixing necessitates the nonorthogonality of ψ_1 and ψ_2. Accounting for overlap, the expression then becomes

$$\Psi = \left(\frac{1}{1 - S\sin 2\delta}\right)^{1/2}(\cos\delta\psi_1 - \sin\delta\psi_2) \tag{8}$$

where S represents the state-to-state overlap between the two diabatic wave functions.

We now consider the basic Hamiltonian for a two level system, introducing an arbitrary coupling term, γ, into the off-diagonal elements.

$$\hat{\mathbf{H}} = \begin{pmatrix} H_1 & \gamma \\ \gamma & H_2 \end{pmatrix} \tag{9}$$

The difficulty in analyzing such a system is in evaluation of γ. However, by applying the wave function described in eq 8 to the Hamiltonian above, we may express γ in terms of more concrete systemic variables, thereby removing it from the problem. In the subsequent section we shall evaluate the explicit adiabatic energy by combining eqs 8 and 9.

Calculation of the Adiabatic Energy. Evaluation of the adiabatic energy by means of eqs 8 and 9 yields the following expression:

$$E_{ad} = \frac{1}{1 - S\sin 2\delta}(E_1\cos^2\delta + E_2\cos^2\delta - 2\gamma S\cos\delta\sin\delta) \tag{10}$$

As γ goes to zero, the system becomes weakly coupled and the final term vanishes. The ground state adiabatic energy will then remain uncoupled and follow the appropriate diabatic paths. For finite γ and S, the final term becomes significant and we must take further steps to evaluate its magnitude.

Fortunately, the geometric characteristics of the symmetric case permit us to greatly simplify eq 10. Because we have defined the energy coordinate such that the crossing occurs at $E = 0$ and assumed that the states evolve linearly, we can express the diabatic energies with great facility:

$$E_1 = E_x\rho$$
$$E_2 = -E_x\rho \tag{11}$$

Substituting eqs 11 into eq 10 and making use of the double angle formula to condense the terms yields:

$$E_{ad} = \frac{1}{1 - S\sin 2\delta}(\rho E_x \cos 2\delta - \gamma S \sin 2\delta) \tag{12}$$

In order to evaluate the magnitude of coupling we must now apply the hyperbolic approximation. In the context of this approximation, the value of the adiabatic energy at the transition state must be equal to $-\alpha E_x$. We now evaluate eq 12 at the transition state ($\rho = 0$, $\delta = \pi/4$) to find the relationship between γ and α.

$$E_{ad}|_{TS} = -\frac{1}{1 - S_{TS}}(\gamma S_{TS})$$
$$= -\alpha E_x$$
$$\gamma = \alpha E_x\left(\frac{1}{S_{TS}} - 1\right) \tag{13}$$

where S_{TS} is the state-to-state overlap evaluated at the transition state. We now have an explicit mathematical relation between the arbitrarily defined coupling constant from the off-diagonal Hamiltonian (γ) and the splitting parameter, α. Equation 13 represents the first critical advancement of the hyperbolic approximation in that it permits us to consider the adiabatic energy in the context of a more quantitatively intuitive coupling term. While α remains an unknown, we may now at least eliminate γ from our energy expression, reducing eq 12 to

$$E_{ad} = \frac{E_x}{1 - S\sin 2\delta}\left(\rho\cos 2\delta - \alpha S\left(\frac{1}{S_{TS}} - 1\right)\sin 2\delta\right) \tag{14}$$

Note that eq 14 applies only to the atom transfer region (Stage II). Outside this region we must treat the reaction in a different coordinate system and ρ is no longer a good variable. However, as this treatment applies only to the near-field, the chosen coordinate system remains valid throughout. Any far-field impacts on the barrier height are encapsulated in the value of E_x; once we have established the energetic and geometric boundary conditions, any changes in barrier height predicted by the model are due to *near-field* effects.

Characterizing the Barrier. In order to achieve our ultimate goal of a solution for α, it is necessary to employ one more energetic relation. We may accomplish this through the applications of basic two-state perturbation theory as described in eq 3 to the derived expression for γ (eq 13). This relation will then permit us to evaluate the splitting at the boundaries as a function of α. The resultant value may then be equated to that of eq 14 at the boundary to yield a solution for α.

According to second-order nondegenerate perturbation theory, splitting to the lower adiabatic surface at $\rho = \pm 1$ is given by

$$E_{splitting} = \frac{(\gamma S_{BC})^2}{\Delta E_{diabatic}}$$
$$= \frac{(\gamma S_{BC})^2}{2E_x}$$

where $E_{splitting}$ is the difference between the diabatic and resultant adiabatic energy at the boundary, and S_{BC} is the diabatic state-to-state overlap evaluated at the boundary. Eliminating γ yields

$$E_{splitting} = E_x\frac{\alpha^2\left(\frac{S_{BC}}{S_{TS}} - S_{BC}\right)^2}{2} \tag{15}$$

We may now combine this fundamental perturbative splitting value with the functional definition of the hyperbola given in eq 4 to derive the following relation.

$$-E_x(\alpha^2 + 1)^{1/2} = -E_x - E_x\frac{\alpha^2\left(\frac{S_{BC}}{S_{TS}} - S_{BC}\right)^2}{2}$$
$$(\alpha^2 + 1)^{1/2} = 1 + \frac{\alpha^2\left(\frac{S_{BC}}{S_{TS}} - S_{BC}\right)^2}{2}$$

Solving for α (which, by definition, is positive and real) yields

$$\alpha = \frac{2S_{TS}(S_{TS}^2 - S_{BC}^2(S_{TS} - 1)^2)^{1/2}}{S_{BC}^2(S_{TS} - 1)^2} \tag{16}$$

Note that the solution selected for eq 16 is the appropriate one for positive values of S_{TS} and S_{BC}. While it is mathematically viable for these quantities to be negative, the α which would result from the appropriately chosen solution (i.e., for $S < 0$) is identical to the value obtained by substituting the absolute value of the state-to-state overlap into the formula above.

This basic solution permits us to predict a near-field barrier height simply by calculating the magnitude of state-to-state overlap at two points along the reaction coordinate. Most significantly, eq 16 identifies state-to-state overlap as the critical driving force in barrier evolution in the near-field and demonstrates that both its absolute value and its functional form are influential. Finally, eq 16 provides us with a quantitative framework within which to consider variation over a series of reactions with similar far-field properties.

Constructing the Diabatic States

As shown in the previous section, the principal quantity driving the evolution of barrier heights in the near-field is the state-to-state overlap. In order to obtain a value for the splitting, it becomes necessary to quantify the state-to-state overlap by characterizing the specific diabatic states involved. Critical to this process is the recognition of the system components most responsible for barrier formation; once these component orbitals have been identified we may further simplify the calculation by examining their energy evolution in isolation. While this assumption of separability is inarguably an approximation, it is certainly reasonable in the context of trend description.

In the near-field representation, transition from reactants to products may be expressed by the transfer of a single electron. As a result, we may separate overall reactant and product wave

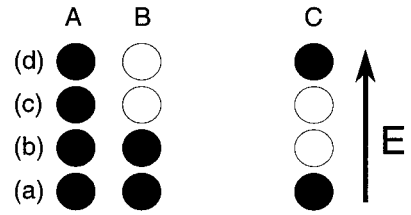

Figure 3. Four configurations (assuming arbitrary positive coefficients) representing every permutation of a linearly arranged three orbital interaction.

functions into a common wave function, ψ_o, and a function representing the singly occupied molecular orbital.

$$\psi_1 = \psi_o\tilde{\psi}_1$$

$$\psi_2 = \psi_o\tilde{\psi}_2 \tag{17}$$

The functions $\tilde{\psi}_1$ and $\tilde{\psi}_2$ are molecular orbitals which correspond to reactant ground state/product excited state and product ground state/reactant excited state respectively, permitting us to consider the reactive system in the context of the frontier molecular orbital analysis, as pioneered by Fukui.[3] If we make the approximation that the near-field barrier is principally attributable to the mixing of $\tilde{\psi}_1$ and $\tilde{\psi}_2$, we may vastly simplify our calculation by looking only at the barrier (and therefore the overlap) arising from these two orbitals.

We may now estimate the barrier height by constructing $\tilde{\psi}_1$ and $\tilde{\psi}_2$ in the context of basic molecular orbital theory and then explicitly calculating the overlap between them:

$$S = \langle\tilde{\psi}_1|\tilde{\psi}_2\rangle \tag{18}$$

By taking advantage of the symmetry characteristics of the system and exploiting known properties of the isolated species, one may constrain the relationships among the coefficients to construct the appropriate diabatic orbitals. As such, the first step in selecting the orbitals of interest is to examine the nature of the individual two-atom interactions involved in bonding.

Consider a set of three atoms, A, B, and C, arranged linearly. To maintain generality, let us assume that the bonding interactions in each species involve a single orbital of unspecified symmetry, designated by ϕ_a, ϕ_b, and ϕ_c respectively. For simplicity, we shall take the ϕ functions to be pure atomic orbitals. We now seek to use this three-orbital system to construct a pair of states which possess the previously specified properties of $\tilde{\psi}_1$ and $\tilde{\psi}_2$. A properly constructed set of orbitals will provide the ideal framework within which to consider atom transfer reactions.

We shall construct these basis states by using a basic linear combination of atomic orbitals (LCAO) technique. Disregarding coefficient values for the moment and considering only phases, there are four fundamental configurations available to the system: all nearest interactions favorable (Figure 3a), a favorable interaction between A and B and a disfavorable interaction between B and C (Figure 3b), a disfavorable interaction between A and B and a favorable interaction between B and C (Figure 3c), and all nearest interactions disfavorable (Figure 3d)

Let us now consider evolution of orbital energetics along the reaction coordinate in the context of an atom transfer reaction, AB + C → A + BC. The relative energy of the orbitals evolve over the atom transfer as indicated in Figure 4. In a three-orbital, three-electron system, the lowest energy state (a) will be doubly occupied throughout and thus is not affected by the occurrence of the atom transfer. The wave function corresponding to this orbital will be absorbed into ψ_o. Similarly, the highest energy state (d) remains unoccupied and also does not participate. As the final electron will preferentially occupy the available state with lowest energy, the critical states involved in the electron transfer are (b) and (c) which map onto the ground state of reactants and products respectively and become degenerate midway along the reaction coordinate. Clearly, orbitals (b) and (c) have the precise properties we are looking for in $\tilde{\psi}_1$ and $\tilde{\psi}_2$.

Having established the qualitative form of $\tilde{\psi}_1$ and $\tilde{\psi}_2$, let us now approach their construction in a more quantitative sense. One may express these molecular orbital functions as a linear combination of the three *two-orbital* interaction wave functions (ψ^{AB}, ψ^{BC}, and ψ^{AC}). Thus

$$\tilde{\psi}_i = \psi_i^{AB} + \psi_i^{BC} + \psi_i^{AC} \tag{19}$$

In contrast to previous methods[21] which have utilized isolated diatomic wave functions to construct composite triatomic states, this approach *restricts* the wave function to two-atom interactions By neglecting the influence of the third atom on the individual diatomic wave functions, eq 19 is able to account for each contributing component without adiabatizing the overall system

For a symmetric atom transfer, A and C are equivalent, and the individual, unnormalized wave functions are given by

$$\psi_1^{AB} = (\phi_a + \chi_{HOMO}\phi_b)$$

$$\psi_1^{BC} = (\chi_{LUMO}\phi_b - \phi_c)$$

$$\psi_1^{AC} = (\phi_a - \phi_C)$$

$$\psi_2^{AB} = (\phi_a - \chi_{LUMO}\phi_b)$$

$$\psi_2^{BC} = -(\chi_{HOMO}\phi_b + \phi_c)$$

$$\psi_2^{AC} = (\phi_a - \phi_c) \tag{20}$$

The coefficients χ_{HOMO} and χ_{LUMO} arise from a simple rearrangement of the molecular orbital coefficients of the isolated diatomic. They are defined such that if the unnormalized solutions for (AB or CB), accounting for conservation of states, are given by

$$\psi_{HOMO} = c_{a,c}\phi_{a,c} + c_b\phi_b$$

$$\psi_{LUMO} = (c_b + s_{(a,c)b}c_{a,c})\phi_{a,c} - (c_{a,c} + s_{(a,c)b}c_b)\phi_b \tag{21}$$

where $s_{(a,c)b}$ is the interatomic overlap between orbitals $\phi_{A,C}$ and ϕ_B, the respective χ terms are defined:

$$\chi_{HOMO} = \left(\frac{c_b}{c_{a,c}}\right)$$

$$\chi_{LUMO} = \left(\frac{(c_{a,c} + s_{ab}c_b)}{(c_b + s_{ab}c_{a,c})}\right) \tag{22}$$

The magnitude of each χ therefore quantifies the relative distribution of electron density in the isolated diatomic molecules for both the bonding and antibonding configurations. The molecular orbital coefficients may be easily estimated based on the charge distribution implied by the molecular dipole moment.

By means of eqs 20−22 and the symmetry requirement which dictates that the coefficients of ϕ_a and ϕ_c must be equal in magnitude, the total, unnormalized molecular orbital wave functions now become

$$\tilde{\psi}_1 = \phi_a + \Xi\phi_b \pm \phi_c$$
$$\tilde{\psi}_2 = \phi_a + \Xi\phi_b \pm \phi_c \qquad (23)$$

where

$$\Xi \equiv \left(\frac{\chi_{HOMO} + \chi_{LUMO}}{2}\right) \qquad (24)$$

Because of the anticorrelation between χ_{HOMO} and χ_{LUMO}, the parameter Ξ may be presumed a constant throughout the near-field for a given chemical system. With the obvious exception of homonuclear diatomics, ground and excited state electron density will shift as the bond is lengthened away from equilibrium, thereby altering both χ values. However, as electron density in the HOMO shifts toward the more electronegative atom, the electron density in the LUMO shifts away from it, keeping the quantity Ξ relatively constant. In fact, even HF, a notoriously problematic and highly polar molecule, shows a variation in Ξ of less than 5% as the bond is stretched from equilibrium to its largest near-field value at the Stage II/Stage III boundary. Clearly, for a homonuclear diatomic χ_{HOMO} and χ_{LUMO} (and therefore Ξ) each reduce to 1.

Equations 23 represent the complete strategy for frontier orbital construction in the symmetric case. Armed with these formulae, we are now equipped to evaluate the state-to-state overlap and thereby quantify the coupling.

State-to-State Overlap and Coupling. Now that we have established a concrete methodology for construction of the frontier molecular orbitals, we are equipped to think more quantitatively about the evolution of the state-to-state overlap over the reaction coordinate. Furthermore, we are in the position to quantify how this important property evolves from system to system.

First, however, we must explicitly calculate the state-to-state overlap. Normalization of eqs 23 yields

$$\tilde{\psi}_1 = N_1(\phi_a + \Xi\phi_b - \phi_c)$$
$$\psi_2 = N_2(\phi_a - \Xi\phi_b - \phi_c)$$
$$N_1 = \left(\frac{1}{2 + \Xi(\Xi + (s_{ab} - s_{bc})) - 2s_{ac}}\right)^{1/2}$$
$$N_2 = \left(\frac{1}{2 + \Xi(\Xi - (s_{ab} - s_{bc})) - 2s_{ac}}\right)^{1/2} \qquad (25)$$

where the $s_{\alpha\beta}$ are the off-diagonal elements of the interatomic overlap matrix. The total state-to-state overlap is given by

$$S = \langle\tilde{\psi}_1|\tilde{\psi}_2\rangle$$
$$= (2 - \Xi^2 - 2s_{ac})(2 + \Xi(\Xi - (s_{ab} - s_{bc})) - 2s_{ac})^{-1/2}(2 + \Xi(\Xi + (s_{ab} - s_{bc})) - 2s_{ac})^{-1/2} \qquad (26)$$

Equation 26 implies that S will change very little over the atom transfer reaction coordinate, as both Ξ and s_{ac} are constant; The only terms which vary are s_{ab} and s_{bc}, but even those effects will be minute because the opposing signs of the terms in the denominator counteract each other, producing only a small variation in S. Figure 5 depicts the variation in total state-to-state overlap with s_{ab} and s_{bc}.

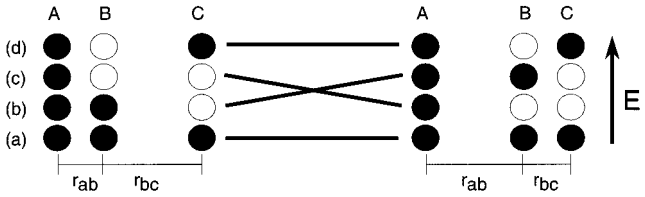

Figure 4. Energy evolution of the four orbital configurations. The lowest (a) and highest (d) energy orbitals maintain their relative energetic locations throughout the atom transfer. Orbitals (b) and (c) invert over the course of the transfer, becoming degenerate at $r_{ab} = r_{bc}$.

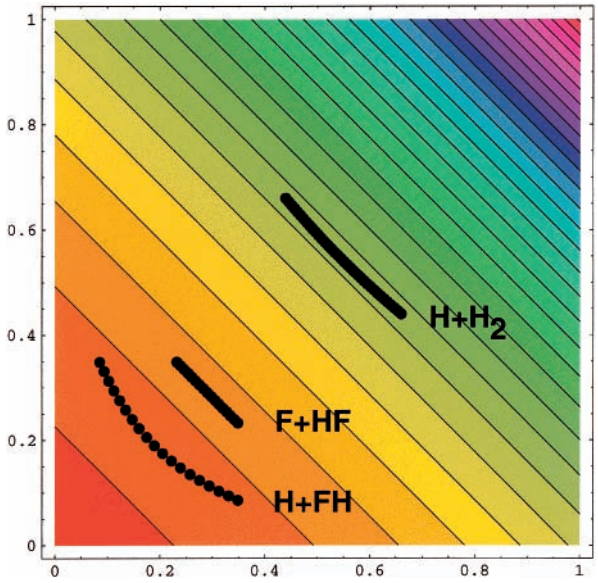

Figure 5. Variation of the total state-to-state overlap as a function of s_{ab} and s_{bc}. The black points represent the locations of the H + H_2, H + FH, and F + HF systems, indicating that the anticorrelation between s_{ab} and s_{bc} results in very little variation in the total state-to-state overlap over the course of the atom transfer. This result suggests that the model may be further simplified by treating the state-to-state overlap as a constant throughout Stage II, requiring its value to be calculated only at the transition state.

Because the two matrix elements s_{ab} and s_{bc} are necessarily anticorrelated in Stage II, chemical systems will tend to evolve parallel to the contour lines depicted in Figure 5. As an example of this behavior, the matrix elements of the H + H_2, H + FH, and F + HF systems (calculated in UHF/STO-3G) have been included in the plot. The reactions clearly proceed along a path of approximately constant state-to-state overlap, so it will vary only slightly over the reaction coordinate in each case.

At the transition state, $s_{ab} = s_{bc}$ and eq 26 reduces to

$$S_{TS} = \frac{(2 - \Xi^2 - 2s_{ac})}{(2 + \Xi^2 - 2s_{ac})} \qquad (27)$$

Because of the tendency of the state-to-state overlap to remain roughly constant, we may take this simplified value to represent the property throughout. Utilizing the approximation that $S_{BC} = S_{TS}$, we may now reduce eq 16 to

$$\alpha = \frac{2(1 - (1 - S_{TS})^2)^{1/2}}{(1 - S_{TS})^2} \qquad (28)$$

As expected, the coupling vanishes in the case of orthogonal diabatic states ($S_{TS} = 0$) and blows up when the states become identical ($S_{TS} = 1$). This final formulation provides a fast and simple method for estimating the coupling and, in combination with eq 27, allows for a quantitative analysis of trends by reducing the problem to two easily determinable parameters: Ξ and s_{ac}.

Discussion

Barrier heights in atom transfer reactions are determined by a combination of far-field and near-field effects. In previous papers[15−17] we have shown how far-field properties may be used to determine the appropriate boundary conditions for treatment of electron transfer in the context of a two-state curve crossing. Analysis of far-field influences on the crossing height has proven to be a useful way of isolating the dominant excited state and thereby explaining the mechanistic motivation for reactivity trends. The purpose of this work has been to develop an analogous model for understanding near-field-driven variation in barrier heights.

In order to model near-field barrier height formation we have chosen to approximate the adiabatic barrier as a hyperbola, produced by means of perturbative splitting from linear diabatic states. By matching the explicit adiabatic energy (eq 14) to the functional form of a hyperbola (eq 4), we have derived a general relation (eq 28) between the splitting parameter, α, and the value of the diabatic state-to-state overlap at the transition state. Quantization of this elusive coupling term in terms of concrete quantum-chemical properties has been one of the historical barricades to understanding of near-field barrier control.

While eq 28 represents a significant step toward understanding the physics which underlie curve-crossing reactions, state-to-state overlap is a less than optimal variable with which to fully understand barrier evolution. In order to consider chemical systems within the context of more intuitive physical properties, we have developed a method of diabatic state construction which permits explicit calculation of the state-to-state overlap via eq 27, demonstrating that it is wholly determined by the far-atom orbital overlap term and the parameter, Ξ, a quantity which reflects the distribution of electron density in the isolated molecular species. Both the interatomic overlap and Ξ are easily calculable and do not rely on high-level electronic structure calculations, providing a convenient method for estimation of coupling.

With all of the aforementioned assumptions in place, a rough adiabatic barrier estimate may be calculated by combining eqs 1, 6, 28, and 27 (reproduced below).

$$E_b = E_x(1 - \beta)$$

$$\beta = 1 + \alpha - (1 + \alpha^2)^{1/2}$$

$$\alpha = \frac{2(1 - (1 - S_{ts})^2)^{1/2}}{(1 - S_{ts})^2}$$

$$S_{ts} = \frac{(2 - \Xi^2 - 2s_{ac})}{(2 + \Xi^2 - 2s_{ac})} \qquad (29)$$

At this level of treatment, a highly accurate barrier height prediction cannot be expected. However, as a mathematical way to explain reactivity trends, this zeroth order model provides a solid foundation.

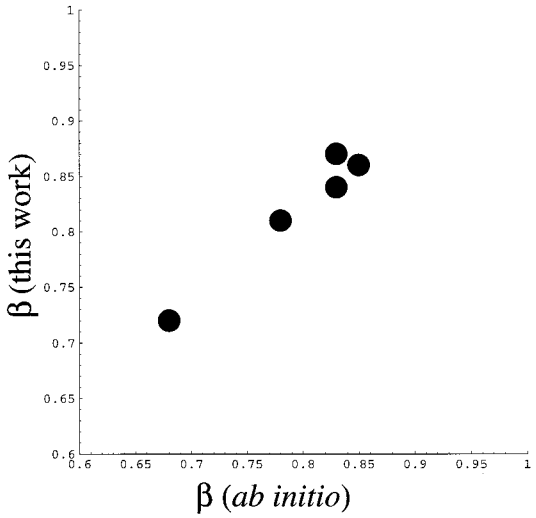

Figure 6. A comparison of the β terms calculated by ab initio theory and those predicted by the model presented in this work.

TABLE 1: Coupling Terms for a Series of Linear, Symmetric Triatomic Reactions As Calculated by ab Initio Methods (UMP2/6-31G) and the Model Presented in This Work**

reaction	β (ab initio)	β (this work)
H + H_2	0.83	0.84
F + HF	0.85	0.86
Cl + HCl	0.83	0.87
H + ClH	0.78	0.81
H + FH	0.68	0.72

Application to a Few Chemical Systems. As a first test of the model's ability to reproduce reactivity trends, we have applied eqs 29 to a few symmetric triatomic systems. Unfortunately, very few experimental data are available for the systems of interest, making evaluation of the model's overall barrier height prediction capacity difficult. However, in lieu of experimental numbers, we have chosen to compare our predictions to ab initio results. While not ideal, this comparison should at least provide a general sense of the model's applicability to trend prediction.

Table 1 lists the nondimensional coupling parameter, β, for a series of reactions as calculated by ab initio (UMP2/6-31G**) and eqs 29. It is significant to note that while the presented results were calculated with the simplest formulation of this model, numbers produced by the more detailed method (eqs 16 and 26) differed by less than 1% in every case. This result is highly encouraging and reconfirms that the approximation of constant state-to-state overlap throughout Stage II is an acceptable one.

Because this basic model makes the assumption of system linearity, the transition states from which we derived the numbers in Table 1 were constrained to their linear forms. Although the "true" transition states of many of the reactions depicted are, in actuality, nonlinear, this fact is immaterial to the validity of the coupling calculation. The effective linear transition states were determined by locating the first-order saddle points in the restricted linear configuration. The effective β parameter was then determined based on the splitting at the boundary and transition state.

A plot of the data from Table 1 is depicted in Figure 6. The plot shows good agreement with ab initio results, both numerically and in the context of trend prediction.

One very interesting element of the data presented above is the set of results for the H atom transfers. Both methods predict

only a small variation in β, supporting the assumption of Donaue et al.[15] that β will remain roughly constant over a series of reactions and hence that H abstraction reactions are driven principally by variations in far-field properties. While this model does an excellent job quantitatively, reproducing the predictions of electronic structure calculations to within 5%, it is important to reiterate that it does not seek to reproduce the accuracy of ab initio techniques. Our aim was to favor simplicity over numerical accuracy, and while the approximations we have made will naturally introduce some degree of error they should not inhibit its intended purpose of trend prediction. Only comparison against experiments can establish the true accuracy and applicability of this model, but the results of this first test are quite promising, and we feel that this method could ultimately be a powerful tool in further understanding the physical phenomena that drive reactivity.

Derivative Approach to Reactivity. As encouraging as the results presented above are with respect to the applicability of this model, it is vital to remain cognizant of the fact that not all barrier variations are driven by the near-field. To get a full picture of the physics which underly a given series of reactions we must take *both* far-field and near-field effects into account. The derivative approach to reactivity, first introduced in Clarke et al.,[17] has been developed for just such a purpose. Because of its value as a means for reactivity analysis we would like to briefly review the basic strategy of the derivative approach and expound upon how it may be used to garner information about the near-field, as well as differentiate between near and far-field influences on the barrier.

The formulation for the adiabatic barrier height presented in eq 1 is particularly useful for distinguishing among regimes of influence because E_x and β are wholly separable, depending on completely independent system properties. Such a feature becomes significant in the derivative approach to chemical reactivity, in which the total derivative in barrier height over a series of reactions may be expanded into a series of partial derivatives with respect to various properties, ζ_i.

$$\frac{dE_b}{drxn} = \sum_i \frac{\partial E_b}{\partial \xi_i}\frac{\partial \xi_i}{\partial rxn} \tag{30}$$

By analyzing the relative magnitude of each term in eq 30 it becomes possible to isolate the most prominent contributing factors to barrier height differences, providing valuable insight into the reaction mechanism.

Taking the partial derivative of eq 1 with respect to an arbitrary property ξ yields

$$\frac{\partial E_b}{\partial \xi} = (1-\beta)\frac{\partial E_x}{\partial \xi} - E_x\frac{\partial \beta}{\partial \xi} \tag{31}$$

However, the separability of β and E_x implies that for a given ξ one of the terms on the rhs of eq 31 will be zero. If ξ is a feature of the near-field, it will have no effect on the crossing height and the first term of eq 31 will vanish. Similarly, if ξ is a far-field property it cannot affect the splitting and the second term will vanish. As a result, eq 30 may be expressed as

$$\frac{dE_b}{drxn} = (1-\beta)\sum_i \frac{\partial E_x}{\partial \xi_i}\frac{\partial \zeta_i}{\partial rxn} - E_x\sum_i \frac{\partial \beta}{\partial \xi_i}\frac{\partial \xi_i}{\partial rxn} \tag{32}$$

Here ζ_i are the set of far-field properties and ξ_i are the set of near-field properties. This separation permits trends in barrier heights to be identified specifically with the regime which generates them. For variations attributable principally to near-field effects (either explicit diabatic state overlap or the parameters which influence it), the first term in eq 32 will be small relative to the second. Similarly, if the variation is driven by far-field effects (energy gap, reaction enthalpy) the first term will be significantly larger. Analysis of a manifold of reactions will permit us to better distinguish between the types of chemical interactions that are governed by the far-field and those which are controlled by the near-field.

Conclusions

An approximate expression (eq 28) has been derived to estimate the magnitude of the splitting in a symmetric linear curve crossing. This expression involves only the state-to-state overlap evaluated at the transition state and thus is not only calculable, but because it does not rely on a wide array of closely correlated parameters its predictions are testable against experimental measurements.

In order to put eq 28 to use we have proposed a method for diabatic state construction out of the three principal atomic orbitals involved in the bonding interactions. Coefficients in the diabatic wave functions are determined based on coefficient ratios of the diabatic/adiabatic states in the far-field. The parameter, Ξ, reflects how the molecular ground and excited states tend to distribute their electron density and has a strong influence on the state-to-state overlap in the near-field.

Initial comparison of this method of coupling strength calculation against ab initio results are very encouraging, confirming that this method can indeed adequately predict reactive trends. While comparison against experimental results should provide the ultimate demonstration of our model's accuracy, results of this first test are highly encouraging.

By breaking the curve-crossing problem down into two independent effects, crossing height and coupling, it becomes possible to separately analyze the respective impact of each regime on reactivity trends. In this way, one may determine whether a difference in barrier heights is principally due to excited state effects or a radical difference between the reactant and product wave functions. Furthermore, because the coupling is independent of crossing height, the latter property alone may be used to determine which of multiple excited states (i.e., singlet−triplet, ionic, etc.) is most crucial in governing reactivity in a given chemical system, thereby lending insight into the mechanism for that particular series of reactions.

With trend description as its ultimate goal, this model permits facile estimation of near-field interaction energy, providing a simple tool for gleaning fundamental mechanistic information with a minimum of computational expense.

Acknowledgment. The authors would like to gratefully acknowledge the NSF (Grant 9977992) for their kind support.

References and Notes

(1) London, F. *Z. Phys.* **1928**, *46*, 455.
(2) Fukui, K.; Fujimoto, H. *Bull. Chem. Soc. Jpn.* **1968**, *41*, 1989.
(3) Fukui, K.; Fujimoto, H. *Bull. Chem. Soc. Jpn.* **1969**, *42*, 3399.
(4) Fujimoto, H.; Yamabe, S.; Fukui, K. *Bull. Chem. Soc. Jpn.* **1971**, *44*, 2936.
(5) Child, M. *Mol. Phys.* **1971**, *20*, 171.
(6) Broeckhove, J.; Claessens, M.; Lathouwers, L.; Deumens, E.; Ohrn, Y.; Van Leuven, P. *J. Chem. Phys.* **1990**, *93*, 8945.
(7) Silver, D. *J. Am. Chem. Soc.* **1974**, *96*, 5959.
(8) Shaik, S.S.; Reddy, A. C. *Trans. Faraday Soc.* **1994**, *90*, 1631.
(9) Shaik, E.; S. Duzy, S.; Bartuv, A. *J. Phys. Chem.* **1990**, *9*, 6574.
(10) Shaik, S.S.; Hiberty, P. C. *Adv. Quantum Chem.* **1995**, *26*, 99.
(11) Pross, A.; Shaik, S.S. *Acc. Chem. Res.* **1983**, *16*, 363.

(12) Pross, A. *Adv. Phys. Org. Chem*. **1985**, *21*, 99.
(13) Pross, A.; Yamataka, H.; Nagase, S. *J. Phys. Org. Chem.* **1991**, *4*, 135.
(14) Yasumori, I. *Bull. Chem. Soc. Jpn.* **1959**, *32*, 1103.
(15) Donahue, N. M.; Clarke, J. S.; Anderson, J. G. *J. Phys. Chem*. **1998**, *10*, 3923.
(16) Clarke, J. S.; Kroll, J. H.; Donahue, N. M.; Anderson, J. G. *J. Phys. Chem*. **1998**, *102*, 9847.
(17) Clarke, J. S.; Rypkema, H. A.; Kroll, J. H.; Donahue, N. M.; Anderson, J. G. *J. Phys. Chem*. **2000**, *104*, 4458.
(18) Shaik, S. S.; Hiberty, P. C.; Lefour, J.-M.; Ohanessian, G. *J. Am. Chem. Soc*. **1987**, *109*, 363.
(19) Cohen-Tannoudji, C.; Diu, B.; Laloe, F. *Quantum Mechanics*; John Wiley and Sons: New York, 1977.
(20) Johnston, H. S.; Heicklen, J. *J. Phys. Chem*. **1966**, *66*, 532.
(21) Yasumori, I. *Bull. Chem. Soc. Jpn.* **1959**, *32*, 1110.